Group: Framatome Professional School

CFD validation of fuel assembly flow

SESAME Deliverable 854935 D2.18

Abdalla Batta, Andreas Class

Introduction

The development and validation of advanced numerical approaches for liquid metal fast reactors is one of the mean objective of SESAME project. The work presented here is a part of work package 2 (WP2) where RANs Models is validated with DNS results generated within SESAME project. The considered case represents flow of liquid metal in infinite heated fuel pin bundle simulator (FPBS). The DNS results (three cases) were presented in [1,2]. The considered geometrical parameters are similar to those used in the fuel pin simulator test section built in the NACIA-UP facility located at ENEA. See [3,4] for more details about the experiment and test cases. Figure 1 shows a sketch of the fuel pin bundle simulator and a picture of the teste section. This fuel pin bundle configuration is relevant for the ALFRED's core thermal-hydraulic design. ALFRED is a flexible fast spectrum research reactor (300 MWth).

The main geometrical dimensions to be considered for a thermal-hydraulic assessment of the FA are:

- The rod diameter D=10 mm;
- The pitch to diameter ratio P/D =1.4,
- The distance between the last rank of pins and the internal wall of the wrap δw= 1.75 mm;
- The regular lattice is triangular/hexagonal staggered;
- The internal hexagonal key of the wrapper is H=62 mm.

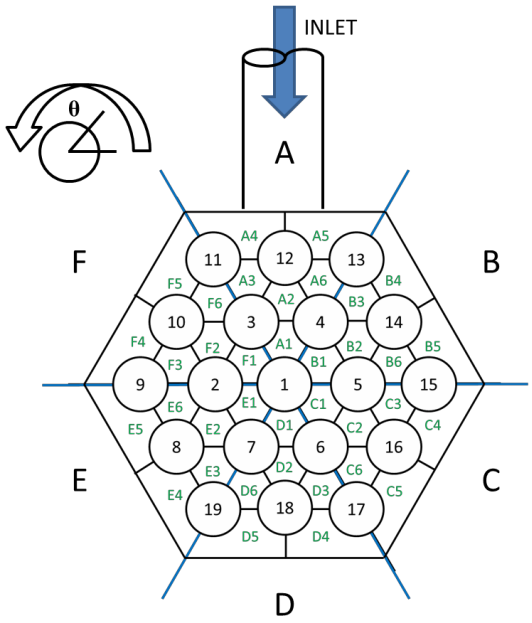

Fig. 1 top view of the fuel pin bundle simulator for the NACIE facility, schematic view (top), actual picture (bottom), [2].

Table 1 summarize the considered cases for DNS study and figure 2 illustrate the considered periodical element. Data are taken from [1,2]. The DNS results were obtained for

Pr=0.31 computed at a reference temperature T_{ref} =220°C. This temperature is consided as the average fluid temperature in the computed domain. The fluid properties are according to [5]. For case 1 and case 2 of table 1 constant wall heat flux of 65.8 kW/m^2. For case 3 the heat flux q" is 131.6 kW/m^2. The gravity is only consider in case 2 where in case 1 and 3 the gravity effect is not considered. The red marked region in figure 2 is considered for the DNS computations. The computational domain size considered is $1.2D_h \times 2.1D_h \times 8\pi D_h$, [2]. The hydraulic diameter (D_h) of the subchannel triangular infinite bundle is given by the following equation

$$D_h = \left[\frac{2\sqrt{3}}{\pi} * \left(\frac{P}{D}\right)^2 - 1\right] D \qquad \text{(Eq. 1)}$$

Using the given geometrical parameters of P/D=1.4 the subchannel hydraulic diameter for the present case is 1.16D. The DNS results are compared to Kirillov et. el correlation [6] in Table 1. Good agreement can be seen for Nusselt number (Nu). The correlation is simplified as follows:

$$Nu = 7.55X - 20/X^{13} + (0.041/X^2)\, Pe^{0.56+0.19X} \qquad \text{(Eq. 2)}$$

Where X=P/D and Pe=Re.Pr. The accuracy of this correlation is estimate by [6] to be 12-15%. This correlation was selected for the comparison, because it represents near average values of many available correlation in literature according to Manservisi [7] comparison.

Table 1. DNS considered cases and resulted Nusselt number.

	Case 1	**Case 2**	**Case3**
Re_τ	550	550	1100
Ri	0	0.25	0
Pr	0.031	0.031	0.031
Re_b	8290	8660	16260
Nu DNS	12.82	12.65	14.79
Nu Kirillov [6]	12.37	12.44	13.89

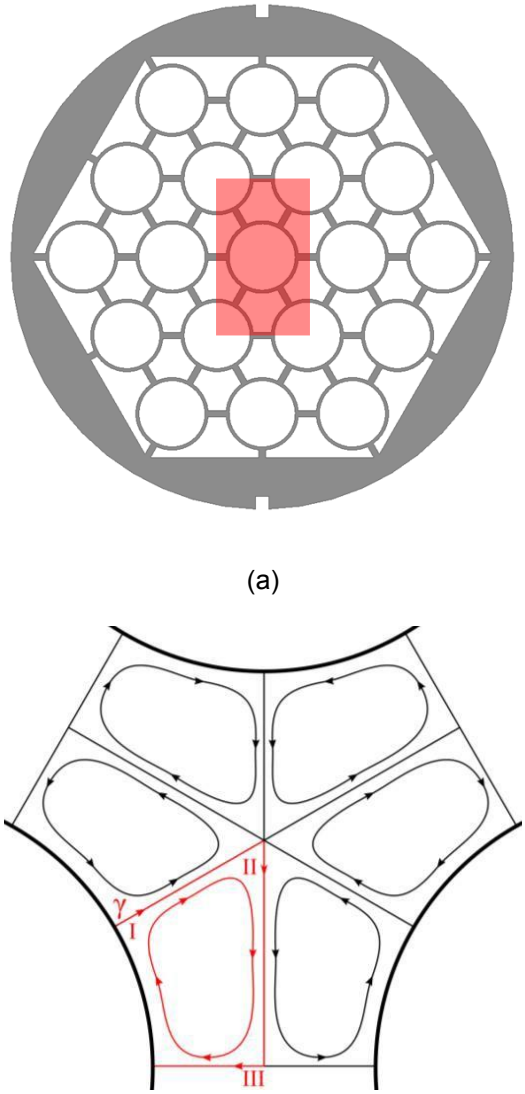

Fig. 2 Periodic module of the NACIE bundle: (a) cross flow layout with periodic rectangular module highlighted, covering four subchannels; (b) unit flow cells, with indication of the curvilinear abscissa γ, defined along its border [2].

In the present work, LBE physical properties, which are all temperature-dependent, are evaluated using empirical correlations suggested in (OECD/NEA Handbook, (2015)). Formulas for density, specific heat, dynamic viscosity, conductivity are reported in Table 2.

Table 2 Physical properties of LBE as a function of temperature (T in Kelvin).

Property	Symbol	Correlation	Maximum Uncertainty	Standard deviation
Density	$\rho(T)$	$11065 - 1.293 \cdot T$	$\leq 0.8\%$	0.58%
Heat capacity	$c_p(T)$	$164.8 - 3.94 \cdot 10^{-2} \cdot T + 1.25 \cdot 10^{-5} \cdot T^2 - 4.56 \cdot 10^{-5} \cdot T^{-2}$	$\leq 5.0\%$	2.4%
Dynamic viscosity	$\mu(T)$	$4.94 \cdot 10^{-4} \exp(754.1/T)$	$\leq 6.0\% - 8.0\%$	7.2%
Thermal conductivity	$k(T)$	$3.284 + 1.67 \cdot 10^{-2} \cdot T - 2.305 \cdot 10^{-6} T^2$	$\leq 10.0\%$ -15.0%	6.2%

In the next section numerical RANs model, computational domain and the numerical Nusselt number results will be presented and compared to the reference DNS results presented above.

Numerical model and results

The selected periodical element shown in figure 2-a is considered for the RANS simulation. An axial length equivalent to the heated length of NACIA experiment is considered, heated length L_h is 0.6 m. Fig. 3 shows the heated walls of the computational domain with the y+ contours for case 1. As it can be seen y+ is selected to be less than 0.5 so that when the higher velocity is considered for case 3 the y+ remains under 1 to satisfy the model needs for low y+ values. Near 5 million cells were used

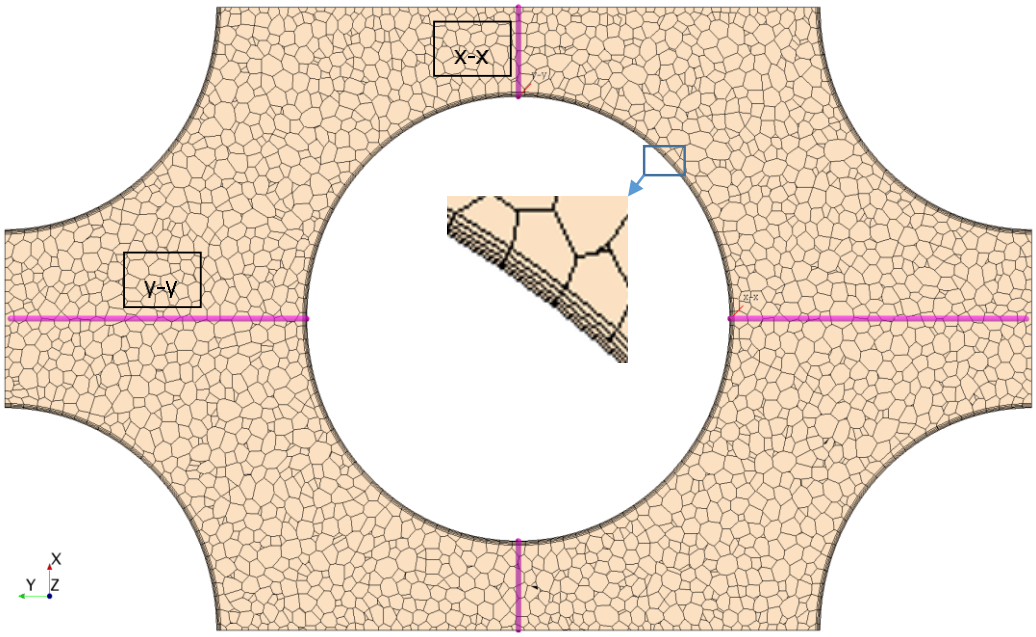

Fig. 4. Mesh and lines through centre plane.

to mesh the domain. Figure 4 shows a cross section of the mesh at the middle of the computational domain. It shows also two lines which will be used in the post processing.

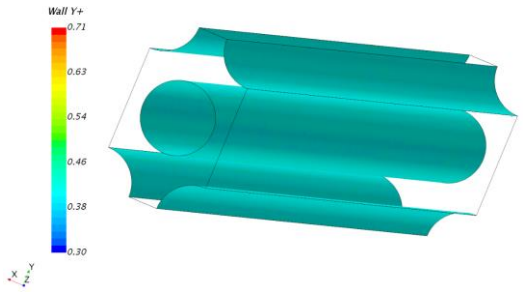

Fig. 3. Y+ values for case 1 and computational domain.

CCM+ is used for the simulation of the current study. The standard k-ε low-Re turbulent model with all y+ wall treatment for steady flow is applied. Fig. 5 shows the velocity contours at inlet and the outlet of the periodical element considered. It shows the walls of the heated rods (0 velocity) one of the rods is not illustrated for purpose of clearness. Local temperature along two lines passing through the center of the computational domain as illustrated in Fig. 4 are plotted in figure 6. It can be seen that, with the considered fine mesh, approximately linear temperature distribution adjacent to the walls can be seen. Temperature contours for case 1 is given in Fig. 7, it shows the temperature contours at inlet, outlet and at rods.

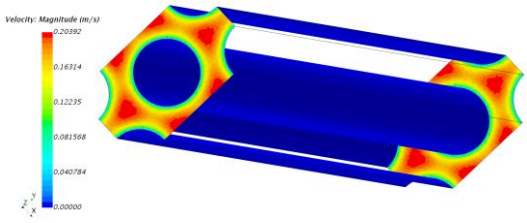

Fig. 5. Velocity contours for case 1. One rod wall is not illustrated for clearness

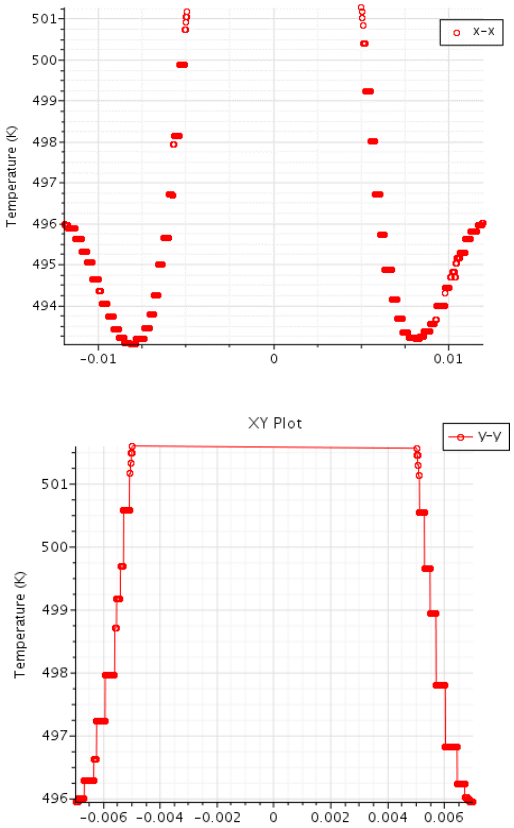

Fig. 6. Temperature along x-x and y-y lines shown in Figure4.

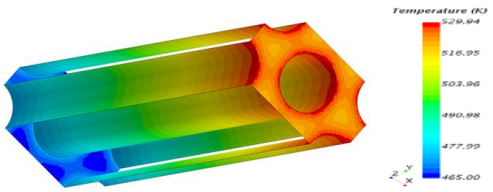

Fig. 7. Temperature contours for case 1, without gravity.

For case 2 and 3 temperature contours are given in Fig. 8 and Fig. 9. Comparing .Fig. 7 for case 1 with figure 8 for case 2, it can be seen that the gravity has very small effect on temperature distribution, so that near similar distribution of temperature as in case 1 was observed. The maximum difference in local temperature was less than 3°C, compare the

scales of Fig. 7 and Fig. 8. Considering case 3, which has double mass flow rate and double heat load as case 1, the temperature contours shown in Fig. 9 shows that case 3 has higher wall temperatures than case1, near 8 °C.

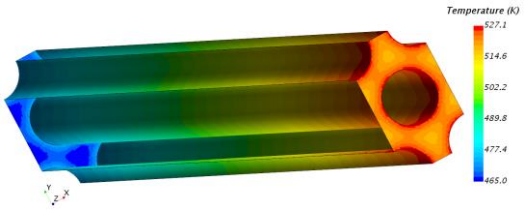

Fig. 8. Temperature contours including gravity, case2.

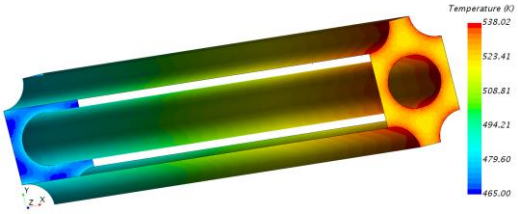

Fig. 9. Temperature contours without gravity, case3.

Comparison of RANs and DNS results

Nusselt number is calculated based on the average wall temperature and average bulk temperature using fluid properties according to table 2 at mean bulk temperature. Table 3 present the numerical results compared to DNS and Kirillov [6] results. The compression of both DNS results and the RANS results give the same qualitative agreement with [6]. The comparison is plotted in figure 10.

Table 3. Nusselt number values compared to DNS and Kirillov[6].

Pe	Ri	DNS	RANs	[6]
257	0	12.82	12.68	12.37
268	0.25	12.65	13.00	12.44
504	0	14.79	14.15	13.89

Conclusion

The numerical study conducted here has compared the heat transfer results obtained from standard RANS model to the DNS results and existing correlation of [6]. The comparison of Nusselt number for all compared cases show a very good agreement with the numerical DNS result and with the literature. Considering the effect of gravity by comparing case 1 and case 2, the resulted temperature distribution looks similar for the given difference of Richardson number(Ri=0.25) . Comparison of case 1 to case 3 which has double mass flow and heat load than case 1 has shown that slight increase in the maximum domain temperature of near 8°C.

Considering the computational domain for periodical element, one could use shorter computational domain since the domain length in z direction shows a periodical behaviour. Considering the velocity distribution in the x-y plane it can be seen that a very smaller periodical element like illustrated in red in figure 2-b could be sufficient for the periodical study.

Nomenclature

Symbol	Quantity	SI Unit
D	Pin diameter	m
D_h	Hydraulic diameter	m
L_h	Heated length	m
H	Hexagonal key of the wrapper	m
Nu	Section average Nusselt number	-
P	Pitch of the bundle	m
p,p_m	Pressure, modified pressure fields	Pa
Pr	Prandtl number	-

q''	Wall heat flux	W/m^2
Re_b	Bulk Reynolds number	-
Re_τ	Reynolds tau number	-
Ri	Richardson number	-
T	Temperature	°C
T_{ref}	Reference temperature difference	°C
T_{bulk}	Bulk temperature	°C
u	Dimensionless velocity component	-
x,y,z	Dimensionless spatial coordinates	-
Greek letters		
δ_w	Distance between the last pin and the wrapper	m
k	Thermal conductivity	W/m/K
μ	Dynamic viscosity	Pa s
ρ	Density	kg/m^3

References

[1] Diego, A., MIXED CONVECTION OF LBE IN THE FUEL PIN BUNDLE OF THE NACIE-UP FACILITY: EXPERIMENTS AND SIMULATIONS SESAME workshop, Petten 2019

[2] Diego, A., Reference data for rod bundle, UNIMORE, SESAME deliverable, D2.6

[3] Di Piazza, I., BFPS Experiment, ENEA, SESAME deliverables, D2.7

[4] Di Piazza, I., Experiment set-up BFPS, ENEA, SESAME deliverables, D2.5

[5] OECD and N. E. Agency, 2015. Handbook on Lead-bismuth Eutectic Alloy and Lead Properties , Materials Compatibility , Thermal- hydraulics and Technologies.

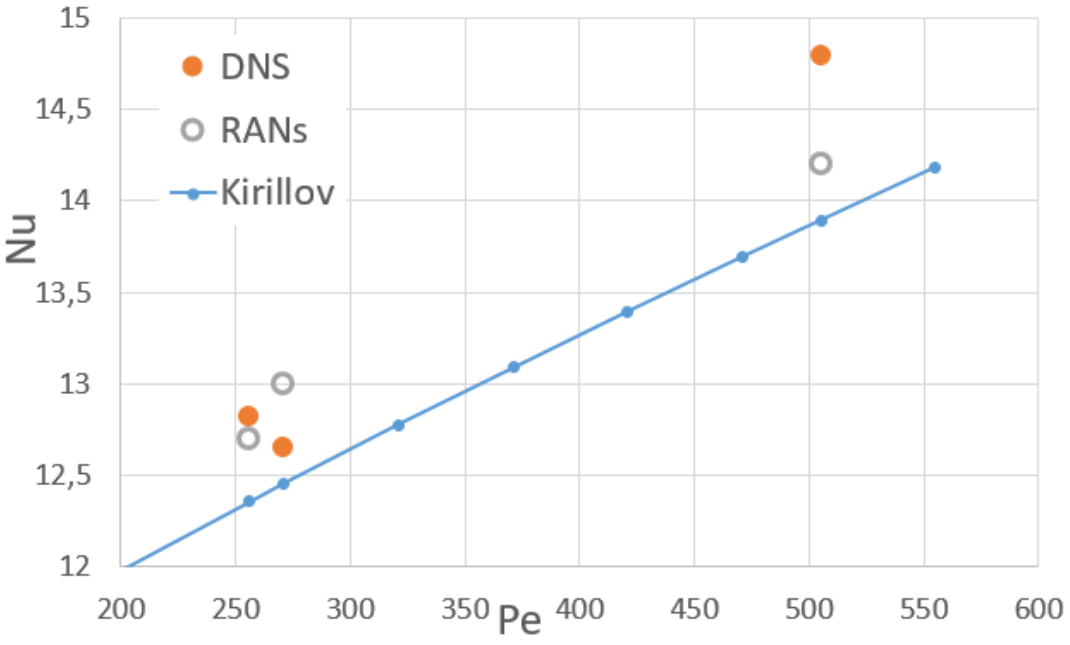

Fig. 10. Nusselt number comparison between RANS results obtained in this study, DNS [1,2] and Kirrillov [6]

[6] Kirillov, P.L. and Ushakov, P.A., 2001. Liquid–metal heat transfer in rod bundles. Thermal Engineering, vol 48, pp.127–133. Marinari, R., Di Piazza, I., Forgione, N., and Magugliani, F., 2017. Pre-test CFD simulations of the NACIE-UP BFPS test section

[7] Manservisi, S. and Menghini, F., Triangular rod bundle simulations of a CFD K-ε-K-Θ -ε-Θ heat transfer turbulence model for heavy liquid metals, Nuclear Engineering and Design 273 (2014) 251–270